VERSITA

Biologia, Bratislava, **61**/Suppl. 18: S51—S64, 2006
Section Zoology
DOI: 10.2478/s11756-006-0119-4

Radiometric dating of sediment records from mountain lakes in the Tatra Mountains

Peter G. Appleby & Gayane T. Piliposian

Department of Mathematical Sciences, University of Liverpool, PO Box 147, Liverpool L69 3BX, United Kingdom; e-mail: appleby@liverpool.ac.uk

Abstract: Sediment cores from nine different lakes in the Tatra Mountains, collected as part of the EU funded AL:PE, MOLAR and EMERGE projects investigating natural environmental records stored in remote mountain lake sediment sequences, were dated radiometrically by ^{210}Pb and ^{137}Cs. At five sites, Długi Staw Gąsienicowy and Zielony Staw Gąsienicowy on the Polish side of the Tatra Mountains and Starolesnianske pleso, Nižné Terianske pleso, and Ľadové pleso on the Slovak side of the Tatra Mountains, the cores were sectioned at close intervals and analysed in detail to produce a high resolution chronology. For the remaining four sites, Zmarzly Staw Gąsienicowy (Poland), and Veľké Hincovo pleso, Vyšné Temnosmrečinské pleso, Vyšné Wahlenbergovo pleso (Slovakia), it was sufficient to establish a low resolution sketch chronology and only a few samples were analysed from each core. At Ľadové pleso, multiple cores were collected in order to establish spatial distribution of sediments over the bed of the lake. Cores from all sites had good records of the fallout radionuclides from which it was possible to construct reliable chronologies of the recent sediments.

Key words: Sediment records, mountain lakes, ^{210}Pb dating, artificial radionuclides, Slovakia, Poland.

Introduction

The main objectives of the recent AL:PE, MOLAR and EMERGE projects (Wathne et al., 1995; Battarbee et al., 2002; http://www.mountain-lakes.org/) were to assess the status of remote mountain lake ecosystems throughout Europe, and make use of their value as sensitive environmental indicators to determine the speed, direction and biological impact of changing air quality and climate. Throughout all three projects, palaeolimnological techniques were widely employed to recover historical environmental data from the high quality records commonly found in lake sediment cores from such relatively remote and undisturbed ecosystems. In carrying out this task it was essential to determine a reliable chronology spanning at least the past century. The principal method used for dating the cores was ^{210}Pb supported by chronostratigraphic dates based on records of the artificial radionuclides ^{137}Cs and ^{241}Am. Following the introduction of the technique by Goldberg (1963) and Krishnaswami et al. (1971), ^{210}Pb has become established as one of the standard tools for dating lake sediments spanning the past 100–150 years. The method is unequivocal at sites where sediment accumulation rates have remained relatively uniform. At such sites concentrations of the unsupported (atmospherically supplied) component of total ^{210}Pb activity decline exponentially with depth at a rate that is inversely proportional to the sedimentation rate. However, at sites impacted by natural and/or anthropogenic environmental change, sedimentation rates may well have varied during this period, causing the unsupported ^{210}Pb concentration versus depth profile to deviate significantly from a simple exponential relationship. Different models have been developed to account for such deviations (Appleby & Oldfield, 1978; Robbins, 1978) and the accuracy of ^{210}Pb dates in a particular application will depend on the validity of the model used. This is usually done by reference to independent records of artificial fallout radionuclides such as ^{137}Cs (Pennington et al., 1973) and ^{241}Am (Appleby et al., 1991) from the atmospheric testing of nuclear weapons or the 1986 Chernobyl reactor accident. A number of techniques for assessing ^{210}Pb data and calculating a best chronology are given in the literature (e.g., Appleby & Oldfield, 1983; Oldfield & Appleby, 1984; Appleby, 2001). One of the key aspects of the ^{210}Pb dating methodology is an assessment of the dominant processes by which fallout is delivered to the core site. A potential problem in dating mountain lakes is the possible impact of seasonal effects on the uniformity of supply rates. During winter the water column is isolated from the natural atmospheric ^{210}Pb flux. Fallout onto the lake and its catchment during this period is locked up in snow and ice and released only at the time of the spring thaw (Piliposian & Appleby, 2003).

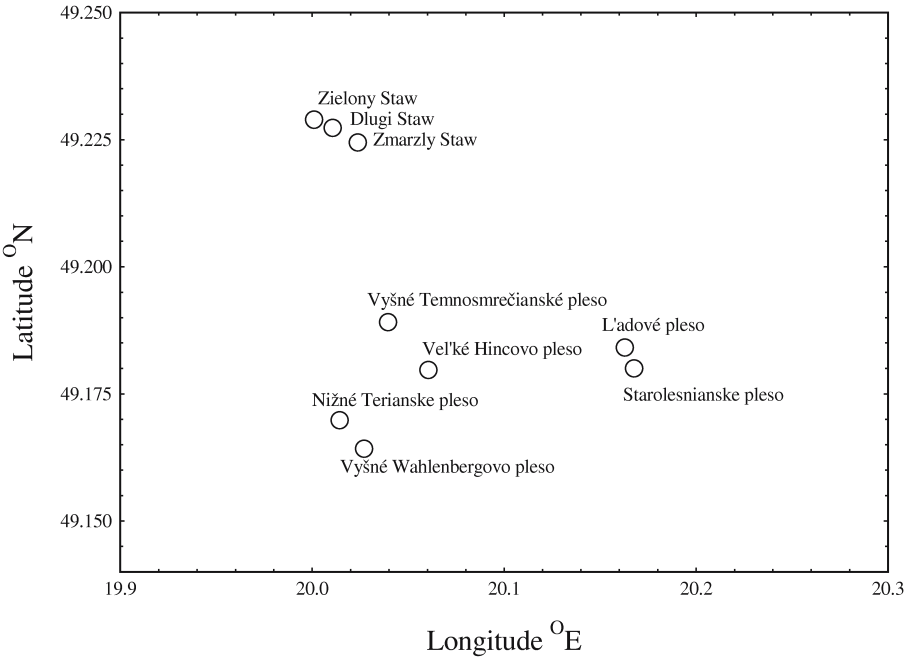

Fig. 1. Diagrammatic site map showing the relative locations of the study lakes.

Table 1. The study sites and their main physiographic parameters.

	Latitude	Longitude	Altitude	Mean annual rainfall	Catch area	Lake area	Max depth	Mean depth
			m a.s.l.	mm y^{-1}	ha	ha	m	m
Poland								
Zielony Staw Gąsienicowy	49°13.7′ N	20°0.1′ E	1672	1161	33.2	3.84	15.1	6.8
Długi Staw Gąsienicowy	49°13.6′ N	20°0.6′ E	1784	1273	39.9	1.59	10.6	5.1
Zmarzly Staw Gąsienicowy	49°13.5′ N	20°1.4′ E	1787	1276	71.9	0.28	3.7	2.3
Slovakia								
Vyšné Temnosmrečinské pleso	49°11.3′ N	20°2.4′ E	1716	1105	112.5	4.51	20.0	10.2
Ľadové pleso	49°11.0′ N	20°9.8′ E	2057	1346	12.9	1.72	18.0	6.7
Starolesnianske pleso	49°10.8′ N	20°10.1′ E	1986	1275	2.3	0.73	4.1	1.5
Veľké Hincovo pleso	49°10.8 N	20°3.6′ E	1946	1235	126.9	18.19	53.2	22.7
Nižné Terianske pleso	49°10.2′ N	20°0.9′ E	1941	1330	91.5	4.91	43.2	17.9
Vyšné Wahlenbergovo pleso	49°9.9′ N	20°1.6′ E	2145	1434	31.9	4.96	21.1	8.5

Problems can also be caused by post-depositional redistribution of ^{210}Pb over the bed of the lake by sediment focussing or slump events. The main objective of this paper is to present a sediment chronology for each core from the study sites that takes account of the possible impact that such processes may have had on the sediment record.

Study sites

The study sites were situated at altitudes ranging from 1672–2145 m a.s.l. within a 10 km × 10 km region of the Tatra Mountains (Mts) bordering Poland and Slovakia ranging from 49°10′–49°14′ N and 20°0′–20°10′ E (Fig. 1). Catchments were all above the local tree-line and composed mainly of stone or gravel with very little vegetation. The lake areas were all quite small (less than 5 ha) apart from Veľké Hincovo pleso, which had an area of 18.2 ha. Mean annual precipitation ranged from 1100–1430 mm y^{-1}. The main physiographic parameters for each site are given in Table 1.

Methods

Sediment cores were collected each site using the methods outlined in Wathne et al. (1995). A list of the cores and the dates of collection is given in Table 2. Those designated as master cores or gradient cores intended primarily for historical reconstructions were sectioned more finely at intervals ranging from 0.25 cm near the top of the core to 1 cm in the deeper sections. Those (from Ľadové pleso) designated as bulk cores and intended primarily for studying the spatial distribution over the bed of the lake were sectioned more coarsely, at intervals ranging from 2 cm near the top of the core to 3 cm in the deeper sections. Sub-samples of dried

Table 2. Tatra lake sediment cores analysed for ^{210}Pb and ^{137}Cs.

Site	Core name	Core date	Type
Zielony Staw Gąsienicowy	ZIEL93/1	1993	Master
Długi Staw Gąsienicowy	DLUG93/1	1993	Master
Zmarzly Staw Gąsienicowy	GA-1	2001	Gradient
Vyšné Temnosmrečinské pleso	TA0019	2001	Gradient
Ľadové pleso	LADO00/1	2000	Bulk
”	LADO00/2	2000	Bulk
”	LADO00/3	2000	Bulk
”	LADO00/4	2000	Bulk
”	LADO00/5	2000	Bulk
”	LADO01/6	2001	Master
Starolesnianske pleso	STAR93/2	1993	Master
Veľké Hincovo pleso	VHINC01/1	2001	Gradient
Nižné Terianske pleso	TERI93/2	1993	Master
”	TERI96/7	1996	Master
Vyšné Wahlenbergovo pleso	FU-1	2001	Gradient

Table 3. Radionuclide parameters for Tatra lake sediment cores.

Core	Unsupported ^{210}Pb						^{137}Cs		^{226}Ra
	Maximum activity		Inventory		Flux		Inventory		Mean activity
	Bq kg^{-1}	±	Bq m^{-2}	±	Bq m^{-2} y^{-1}	±	Bq m^{-2}	±	Bq kg^{-1}
ZIEL93/1	1409	52	9965	238	310	8	4725	110	68
DLUG93/1	1164	54	2185	72	68	2	2207	47	56
GA-1	394	24	2596	190	81	7	4073	130	45
TA0019	1742	67	4766	256	148	8	2565	97	67
LADO00/1	501	22	1584	89	49	3	2174	66	35
LADO00/2	780	28	4427	186	138	6	5858	182	35
LADO00/3	712	27	3699	162	115	5	4704	130	34
LADO00/4	167	13	5388	288	168	8	6394	171	30
LADO00/5	461	22	2227	129	69	5	3291	98	30
LADO01/6	1300	52	3727	113	116	4	4234	82	42
STAR93/2	1229	48	4148	108	129	3	10685	212	40
VHINC01/1	2366	50	11212	654	349	20	12480	498	90
TERI93/2	2623	150	3132	115	98	4	3476	90	53
TERI96/7	2049	94	2760	83	86	3	3121	65	51
FU-1	715	26	1950	122	61	4	4250	164	41
Mean values	1500†		4454		139		4765‡		48

Key: † Excluding the bulk sediment cores; ‡ Decay corrected to a common date of 2000.

sediment from each core were sent to the University of Liverpool Environmental Radioactivity Research Centre where they were analysed for ^{210}Pb, ^{226}Ra, ^{137}Cs and ^{241}Am by direct gamma assay using Ortec HPGe GWL series well-type coaxial low background intrinsic germanium detectors (Appleby et al., 1986). ^{210}Pb was determined *via* its gamma emissions at 46.5 keV, and ^{226}Ra by the 295 keV and 352 keV γ-rays emitted by its daughter isotope ^{214}Pb following 3 weeks storage in sealed containers to allow radioactive equilibration. ^{137}Cs and ^{241}Am were measured by their emissions at 662 keV and 59.5 keV, respectively. The absolute efficiencies of the detectors were determined using calibrated sources and sediment samples of known activity. Corrections to these efficiencies were made for the effects of self-absorption of low energy γ-rays within the sample and different sample heights (Appleby et al., 1992; Appleby & Piliposian, 2004). Radiometric dates were calculated from the ^{210}Pb and ^{137}Cs records using the procedures described in Appleby (2001).

Results

Table 3 summarises a number of radiometric parameters determined for each core. Supported ^{210}Pb in each sample was assumed to be in equilibrium with the *in situ* ^{226}Ra, and unsupported ^{210}Pb calculated by subtracting ^{226}Ra activity from total ^{210}Pb. Radiometric inventories were calculated by numerically integrating the activity versus depth profiles with regard to the cumulative dry mass.

The ^{210}Pb flux is the mean supply rate needed to sustain the measured unsupported ^{210}Pb inventory. The average value over all sites (139 Bq m^{-2}y^{-1}) is signif-

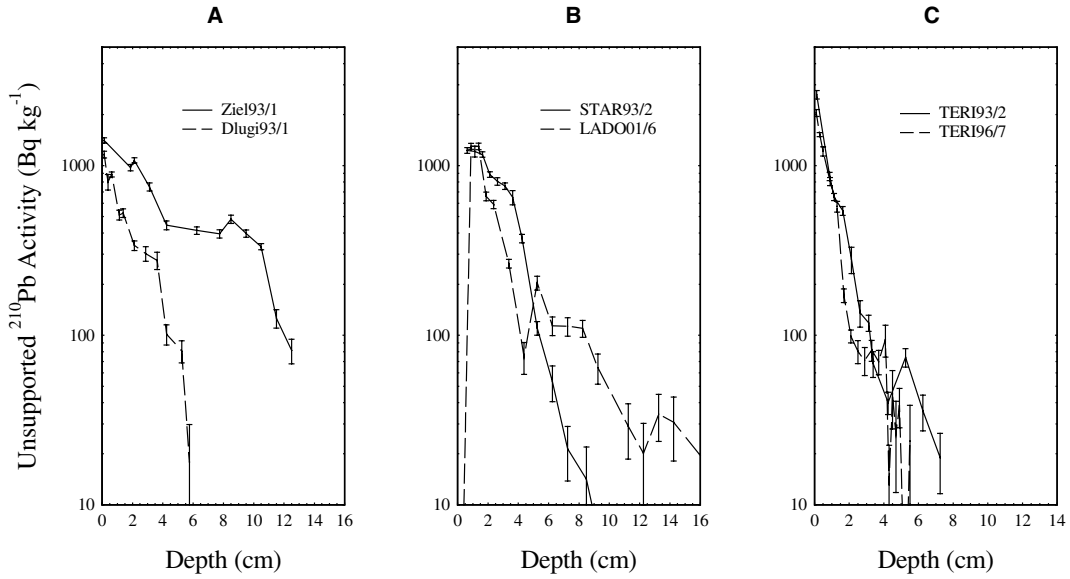

Fig. 2. Fallout ^{210}Pb records in Tatra lake sediment cores showing unsupported ^{210}Pb concentrations versus depth in Zielony Staw Gąsienicowy and Długi Staw Gąsienicowy (A), Starolesnianske pleso and Ľadové pleso (B), and Nižné Terianske pleso (C).

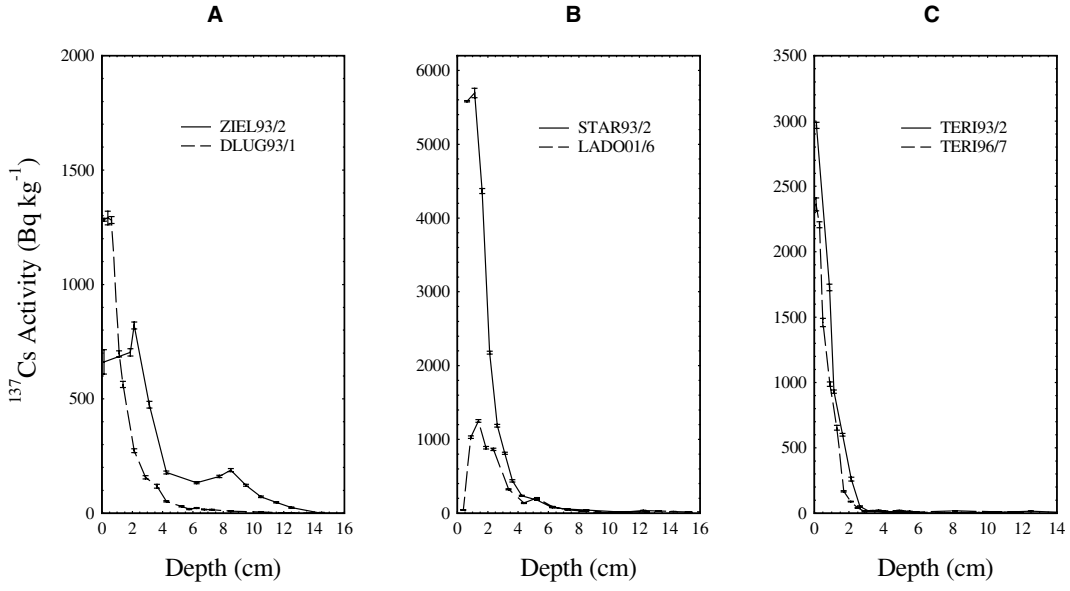

Fig. 3. Fallout ^{137}Cs records in Tatra lake sediment cores showing ^{137}Cs concentrations versus depth in Zielony Staw Gąsienicowy and Długi Staw Gąsienicowy (A), Starolesnianske pleso and Ľadové pleso (B), and Nižné Terianske pleso (C).

icantly lower than the estimated atmospheric flux in this region of between 200–220 Bq m^{-2}y^{-1} (Plöger, 2005), suggesting that a significant fraction of the fallout ^{210}Pb is lost from the lakes, possibly during the spring thaw. The mean ^{137}Cs inventory of 4765 Bq m^{-2} is also significantly lower than the fallout value determined from soil cores at Ľadové pleso of 7149 Bq m^{-2} (Plöger, 2005). At most sites the ^{137}Cs/^{210}Pb inventory ratio is though similar to that in direct fallout, suggesting that ^{137}Cs losses are comparable to those of ^{210}Pb. The high inventories (and fluxes) in Zielony Staw Gąsienicowy and Veľké Hincovo pleso are almost certainly due to sediment focussing at the core sites. The significantly higher ^{137}Cs/^{210}Pb ratios at Starolesnianske pleso and Zmarzly Staw Gąsienicowy can be attributed to higher Chernobyl fallout at these sites. The high surficial ^{210}Pb activities (excluding the bulk cores because of their coarse sectioning) show that all of these lakes have relatively low primary sedimentation rates. Higher net sedimentation rates at individual core sites will most probably be due to processes such as sediment focussing or slumping.

Master cores

In the master cores where the ^{210}Pb records were determined in detail, the depths at which total ^{210}Pb ac-

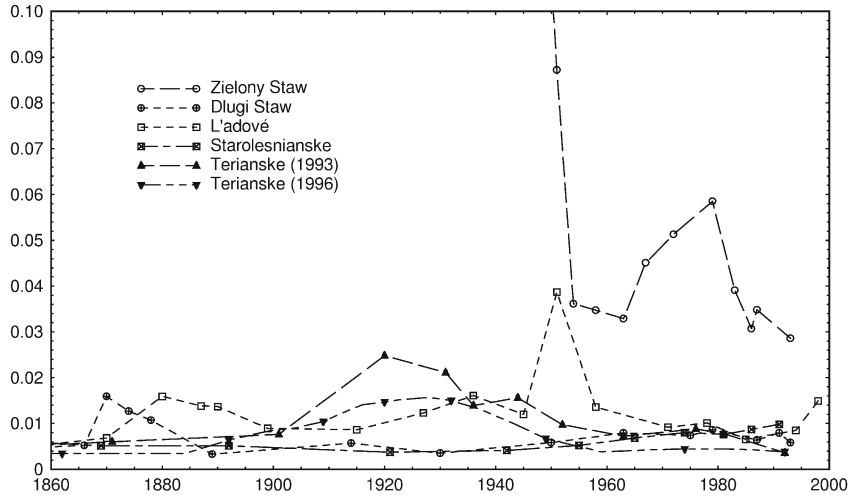

Fig. 4. Sedimentation rates versus time in Tatra lake sediment cores.

Table 4. ^{210}Pb chronology of Zielony Staw Gąsienicowy core ZIEL93/1.

Depth		Chronology			Sedimentation Rate		
		Date	Age				
cm	g cm^{-2}	AD	y	±	g cm^{-2} y^{-1}	cm y^{-1}	±(%)
0.0	0.00	1993	0	0			
0.5	0.04	1992	1	1	0.030	0.31	8.2
1.0	0.09	1990	3	2	0.032	0.32	8.6
1.5	0.14	1989	4	2	0.034	0.33	9.0
2.0	0.19	1987	6	2	0.033	0.29	9.3
2.5	0.26	1985	8	2	0.034	0.25	9.8
3.0	0.32	1983	10	2	0.038	0.26	10.7
3.5	0.40	1981	12	2	0.046	0.29	11.3
4.0	0.48	1980	13	2	0.054	0.32	11.9
4.5	0.57	1978	15	2	0.058	0.33	12.4
5.0	0.65	1976	17	2	0.056	0.32	12.9
5.5	0.74	1975	18	2	0.054	0.31	13.3
6.0	0.83	1973	20	2	0.052	0.29	13.7
6.5	0.92	1971	22	3	0.050	0.28	14.4
7.0	1.01	1969	24	3	0.048	0.27	15.2
7.5	1.10	1968	25	3	0.046	0.25	16.0
8.0	1.19	1965	28	4	0.041	0.23	17.0
8.5	1.29	1963	30	4	0.033	0.19	18.1
9.0	1.37	1961	32	4	0.034	0.21	19.3
9.5	1.44	1958	35	5	0.035	0.22	20.5
10.0	1.52	1956	37	5	0.035	0.23	21.9
10.5	1.60	1954	39	6	0.036	0.23	23.3
11.0	1.68	1953	40	6	0.062	0.38	25.6
11.5	1.76	1951	42	6	0.087	0.54	28.0
12.0	1.84	1950	43	7	0.11	0.47	29.5
12.5	1.93	1949	44	7	0.13	0.41	31.1

tivity reached equilibrium with that of the supporting ^{226}Ra (normally corresponding to around 130 years accumulation) ranged from 6 to 16 cm. Several of the unsupported ^{210}Pb concentration versus depth profiles (Fig. 2) decline in a step-wise manner, with simple exponential sections recording periods of uniform sedimentation separated by irregular features that probably record episodes of rapid sedimentation due e.g. to land-slips from adjacent slopes or sediment slumps. The very low activity in the surficial sediments of the Ľadové pleso master core (Fig. 2B) are presumably due a slide of inorganic material from the catchment that has not recently been exposed to atmospheric fallout.

Figure 3 plots the records of fallout ^{137}Cs in each of the master cores. Only the Zielony Staw Gąsienicowy core (Fig. 3A) has two distinct peaks (at depths of ∼2 cm and 8.5 cm) that can be clearly identified as records of the 1986 Chernobyl accident and the 1963 fallout maxima from atmospheric testing of nuclear weapons. High ^{137}Cs concentrations in the near surface sediments of the other cores are attributable to Cher-

Table 5. ^{210}Pb chronology of Długi Staw Gąsienicowy core DLUG93/1.

Depth		Chronology			Sedimentation Rate		
		Date	Age				
cm	g cm^{-2}	AD	y	±	g cm^{-2} y^{-1}	cm y^{-1}	±(%)
0.00	0.00	1993	0	0			
0.25	0.01	1992	1	2	0.0068	0.12	8.3
0.50	0.03	1989	4	2	0.0072	0.08	8.3
0.75	0.05	1985	8	2	0.0069	0.06	5.9
1.00	0.08	1981	12	2	0.0080	0.07	7.3
1.25	0.11	1977	16	2	0.0080	0.07	7.9
1.50	0.15	1973	20	2	0.0075	0.06	8.0
1.75	0.18	1969	24	2	0.0076	0.06	8.5
2.00	0.21	1965	28	2	0.0078	0.06	9.0
2.25	0.24	1961	32	2	0.0075	0.06	9.9
2.50	0.27	1956	37	2	0.0069	0.06	11.1
2.75	0.30	1952	41	3	0.0062	0.05	12.4
3.00	0.33	1947	46	3	0.0054	0.05	13.6
3.25	0.36	1940	53	3	0.0047	0.04	15.0
3.50	0.39	1934	59	4	0.0039	0.03	16.3
3.75	0.42	1927	66	5	0.0039	0.03	18.2
4.00	0.45	1920	73	5	0.0048	0.04	20.8
4.25	0.47	1914	79	6	0.0057	0.05	23.4
4.50	0.50	1907	86	8	0.0051	0.05	27.9
4.75	0.53	1901	92	9	0.0045	0.04	32.5
5.00	0.56	1895	98	11	0.0039	0.04	37.1
5.25	0.59	1889	104	13	0.0033	0.03	41.7
5.50	0.61	1883	110	15	0.0070	0.06	62.9
5.75	0.64	1878	115	17	0.011	0.10	84.2
6.00	0.67	1876	117	18	0.012	0.10	91.5
6.25	0.70	1874	119	18	0.013	0.11	98.8
6.50	0.73	1872	121	19	0.014	0.12	87.0
6.75	0.76	1870	123	19	0.016	0.14	75.1
7.00	0.79	1868	125	21	0.011	0.09	79.5
7.25	0.82	1866	127	24	0.0052	0.04	83.8
7.50	0.85	1859	134	25	0.0048	0.04	82.5
7.75	0.88	1852	141	26	0.0045	0.04	81.2
8.00	0.91	1845	148	27	0.0041	0.03	79.9
8.25	0.94	1838	155	28	0.0038	0.03	78.6
8.50	0.97	1831	162	29	0.0034	0.03	77.3

nobyl fallout. Since in all these cases the 1963 depth occurs at no more than 3 cm, the earlier (weapons fallout) peak has presumably been masked by downward migration of Chernobyl ^{137}Cs. In Ľadové pleso, Starolesnianske pleso and Nižné Terianske pleso, the approximate 1963 depth was however independently determined by the presence of traces of ^{241}Am, also a product of weapons test fallout (Appleby et al., 1991).

The radiometric records for the master cores are given in full in Tables A1–A6 in the Appendix to this paper.

Radiometric dates and sedimentation rates for each core were calculated using the methods described in Appleby (2001). Sedimentation rates versus time since the mid-19th century, plotted in Fig. 4, suggest that at most sites there is a very low but relatively uniform base-line sedimentation rate of less than 0.01 g cm^{-2} y^{-1}, punctuated by occasional episodes of more rapid accumulation due to land slips from the catchment or sediment slumps within the lake.

Zielony Staw Gąsienicowy

Although ^{210}Pb/^{226}Ra equilibrium in this core is apparently reached at a depth of about 14 cm, the rapid decline in unsupported ^{210}Pb activity below 11 cm (Fig. 2A) occurs just above a layer of dense sediment extending from 13–18 cm, probably caused by a specific event such as a large land-slip that may have destroyed the early part of the ^{210}Pb record. This is supported by the fact that the raw CRS model ^{210}Pb date of the weapons test fallout ^{137}Cs peak at 8.5 cm depth (Fig. 3A) is significantly earlier than its known date of 1963. Revised ^{210}Pb dates calculated using the 1963 peak as a reference point are in good agreement with both ^{137}Cs dates. The results, given in Table 4, date the hiatus in the ^{210}Pb record caused by the dense layer between 13–18 cm to the period 1945–1950. The presence of a second dense layer between 20–27 cm suggests that this particular core site is prone to disruption by episodic land-slips. Although sediments below ca. 12 cm cannot be dated by ^{210}Pb, the presence of traces of unsupported ^{210}Pb in the interven-

Table 6. ^{210}Pb chronology of Ľadové pleso core LAD01/6.

Depth		Chronology			Sedimentation Rate		
		Date	Age				
cm	g cm^{-2}	AD	y	±	g cm^{-2} y^{-1}	cm y^{-1}	±(%)
0.00	0.00	2001	0	0			
0.25	0.03	1999	2	1	0.0149	0.130	4.0
0.50	0.06	1997	4	2	0.0133	0.111	4.4
0.75	0.09	1995	6	2	0.0101	0.086	4.8
1.00	0.12	1992	9	2	0.0081	0.073	5.1
1.25	0.15	1988	14	2	0.0070	0.064	5.3
1.50	0.18	1984	18	2	0.0074	0.063	5.8
1.75	0.22	1980	22	2	0.0092	0.067	6.6
2.00	0.25	1976	25	2	0.0099	0.071	7.0
2.25	0.28	1973	29	2	0.0094	0.074	7.0
2.50	0.31	1970	32	2	0.0097	0.074	7.1
2.75	0.35	1966	35	2	0.0108	0.077	7.3
3.00	0.38	1963	39	2	0.0119	0.077	7.5
3.25	0.42	1960	42	2	0.0130	0.091	7.7
3.50	0.46	1957	45	2	0.0166	0.111	9.5
3.75	0.50	1955	46	2	0.0229	0.125	13.1
4.00	0.53	1954	48	2	0.0292	0.154	16.7
4.25	0.57	1952	50	2	0.0354	0.154	20.2
4.50	0.60	1950	51	2	0.0350	0.154	20.6
4.75	0.64	1949	53	2	0.0274	0.154	17.5
5.00	0.67	1947	54	2	0.0197	0.143	14.4
5.25	0.70	1945	56	2	0.0120	0.125	11.2
5.50	0.73	1943	58	2	0.0130	0.118	12.1
5.75	0.77	1941	61	3	0.0141	0.111	12.9
6.00	0.80	1939	63	3	0.0151	0.105	13.7
6.25	0.83	1936	65	3	0.0161	0.111	14.6
6.50	0.86	1934	68	3	0.0152	0.111	14.8
6.75	0.89	1932	70	3	0.0142	0.111	15.0
7.00	0.92	1930	72	3	0.0133	0.105	15.2
7.25	0.95	1927	74	3	0.0123	0.095	15.4
7.50	0.99	1924	77	3	0.0114	0.087	15.6
7.75	1.02	1921	80	4	0.0105	0.080	15.8
8.00	1.05	1918	83	4	0.0095	0.074	16.0
8.25	1.08	1915	87	4	0.0086	0.069	16.2
8.50	1.12	1911	91	5	0.0087	0.065	18.7
8.75	1.15	1907	95	5	0.0087	0.063	21.1
9.00	1.19	1903	99	5	0.0088	0.071	23.6
9.25	1.22	1899	103	6	0.0089	0.080	26.0
9.50	1.25	1897	105	6	0.0101	0.095	26.9
9.75	1.28	1894	107	6	0.0113	0.118	27.7
10.00	1.32	1892	109	6	0.0125	0.133	28.5
10.25	1.35	1890	111	6	0.0137	0.182	29.4
10.50	1.37	1889	112	6	0.0137	0.250	32.1
10.75	1.40	1889	113	6	0.0137	0.333	34.8
11.00	1.43	1888	113	6	0.0137	0.286	37.5
11.25	1.46	1887	114	6	0.0138	0.200	40.3
11.50	1.48	1886	116	7	0.0143	0.154	43.7
11.75	1.51	1884	118	7	0.0148	0.143	47.2
12.00	1.54	1882	120	7	0.0154	0.125	50.7
12.25	1.56	1880	121	7	0.0159	0.118	54.1
12.50	1.59	1878	124	7	0.0137	0.105	50.4
12.75	1.62	1875	126	8	0.0114	0.095	46.6
13.00	1.64	1872	129	8	0.0091	0.077	42.9
13.25	1.67	1870	132	8	0.0068	0.063	39.1
13.50	1.70	1865	137	9	0.0061	0.056	41.9
13.75	1.72	1859	142	10	0.0054	0.049	44.8
14.00	1.75	1854	147	10	0.0047	0.049	47.7
14.25	1.78	1849	152	11	0.0040	0.048	50.5
14.50	1.81	1844	157	11	0.0044	0.048	50.9
14.75	1.84	1838	163	11	0.0047	0.048	51.4
15.00	1.87	1833	168	12	0.0051	0.046	51.8
15.25	1.90	1828	173	12	0.0055	0.046	52.2
15.50	*1.93*	*1822*	*179*	*13*	*0.0055*	*0.045*	*52.4*
15.75	*1.96*	*1816*	*185*	*14*	*0.0055*	*0.043*	*52.6*

Table 6. (continued).

Depth		Chronology			Sedimentation Rate		
		Date	Age				
cm	g cm^{-2}	AD	y	±	g cm^{-2} y^{-1}	cm y^{-1}	±(%)
16.00	*1.99*	*1811*	*190*	*15*	*0.0055*	*0.041*	*52.8*
16.25	*2.02*	*1805*	*196*	*17*	*0.0055*	*0.039*	*53.0*
16.50	*2.06*	*1798*	*203*		*0.0055*	*0.038*	
16.75	*2.10*	*1791*	*210*		*0.0055*	*0.037*	
17.00	*2.14*	*1785*	*216*		*0.0055*	*0.038*	

NB: Extrapolated dates, shown in italics, have been calculated using the estimated pre-1830 sedimentation rate of 0.0055 g cm^{-2} y^{-1}.

Table 7. ^{210}Pb chronology of Starolesnianske pleso core STAR93/2.

Depth		Chronology			Sedimentation Rate		
		Date	Age				
cm	g cm^{-2}	AD	y	±	g cm^{-2} y^{-1}	cm y^{-1}	±(%)
0.00	0.00	1993	0	0			
0.25	0.01	1992	1	2	0.0100	0.19	4.8
0.50	0.02	1991	2	2	0.0099	0.18	4.8
0.75	0.03	1990	3	2	0.0096	0.16	5.5
1.00	0.05	1988	5	2	0.0090	0.12	7.0
1.25	0.07	1985	8	2	0.0084	0.093	7.1
1.50	0.10	1982	11	2	0.0079	0.081	5.6
1.75	0.12	1979	14	2	0.0077	0.074	4.9
2.00	0.15	1976	17	2	0.0079	0.071	5.1
2.25	0.18	1972	21	2	0.0077	0.066	5.5
2.50	0.21	1968	25	2	0.0071	0.058	6.2
2.75	0.24	1963	30	2	0.0064	0.051	6.6
3.00	0.27	1957	36	2	0.0056	0.045	6.7
3.25	0.30	1952	41	2	0.0049	0.040	7.8
3.50	0.33	1946	47	2	0.0047	0.041	6.4
3.75	0.36	1939	54	2	0.0047	0.038	6.4
4.00	0.39	1933	60	3	0.0047	0.037	6.4
4.25	0.43	1926	67	3	0.0047	0.037	6.4
4.50	0.46	1919	74	3	0.0047	0.038	6.4
4.75	0.49	1913	80	4	0.0047	0.039	6.4
5.00	0.52	1906	87	5	0.0047	0.039	6.4
5.25	0.55	1900	93	5	0.0047	0.039	6.4
5.50	0.58	1893	100	6	0.0047	0.040	6.4
5.75	0.61	1887	106	7	0.0047	0.040	6.4
6.00	0.64	1881	112	8	0.0047	0.040	6.4
6.25	0.67	1875	118	8	0.0047	0.040	6.4
6.50	0.70	1868	125	10	0.0047	0.039	6.4
6.75	0.73	1862	131	11	0.0047	0.039	6.4
7.00	0.76	1856	137	12	0.0047	0.039	6.4
7.25	0.79	1849	144	14	0.0047	0.040	6.4
7.50	0.82	1843	150	16	0.0047	0.040	6.4
7.75	0.85	1837	156	17	0.0047	0.040	6.4
8.00	0.88	1831	162	19	0.0047	0.040	6.4
8.25	0.91	1824	169	21	0.0047	0.040	6.4
8.50	0.94	1818	175	23	0.0047	0.040	6.4

ing layer of apparently normal sediment at 18–19 cm suggests that these events are relatively recent. Since the early 1950s sedimentation rates do however appear to have been relatively uniform, though with a mean value of 0.042 ± 0.005 g cm^{-2} y^{-1} (0.27 cm y^{-1}) that is significantly higher than at the other sites shown in Fig. 4.

Długi Staw Gąsienicowy

The ^{210}Pb dates for this core are relatively unambiguous. Apart from a brief episode of apparently rapid accumulation ca. 1870, sedimentation rates appear to have been relatively uniform since the early 19$^{\text{th}}$ century, with a mean value of 0.0062 ± 0.0003 g cm^{-2} y^{-1} (0.055 cm y^{-1}). The results are given in detail in

Table 8. ^{210}Pb chronology of Nižné Terianske pleso core TERI93/2.

Depth		Chronology			Sedimentation Rate		
		Date	Age				
cm	g cm^{-2}	AD	y	±	g cm^{-2} y^{-1}	cm y^{-1}	±(%)
0.00	0.00	1993	0	0			
0.25	0.01	1991	2	2	0.0043	0.058	6.8
0.50	0.03	1987	6	2	0.0057	0.066	6.9
0.75	0.05	1983	10	2	0.0071	0.074	7.0
1.00	0.08	1979	14	2	0.0083	0.063	7.0
1.25	0.13	1973	20	2	0.0084	0.044	7.4
1.50	0.18	1967	26	2	0.0076	0.039	8.3
1.75	0.22	1961	32	2	0.0078	0.040	11.2
2.00	0.27	1955	38	2	0.0091	0.047	16.3
2.25	0.32	1950	43	3	0.0111	0.056	19.0
2.50	0.37	1946	47	3	0.0141	0.066	19.2
2.75	0.42	1942	51	3	0.0152	0.067	18.2
3.00	0.48	1938	55	3	0.0143	0.058	15.9
3.25	0.55	1934	59	4	0.0174	0.061	17.4
3.50	0.62	1930	63	4	0.0216	0.072	20.3
3.75	0.70	1926	67	4	0.0227	0.078	20.3
4.00	0.78	1923	70	4	0.0237	0.083	20.4
4.25	0.86	1920	73	5	0.0248	0.089	20.4
4.50	0.92	1915	78	5	0.0205	0.075	21.6
4.75	0.98	1911	82	6	0.0162	0.061	22.7
5.00	1.04	1906	87	7	0.0119	0.047	23.9
5.25	1.11	1901	92	7	0.0076	0.033	25.0
5.50	1.16	1894	99	10	0.0072	0.033	32.7
5.75	1.21	1886	107	12	0.0068	0.032	40.4
6.00	1.27	1878	115	14	0.0064	0.032	48.0
6.25	1.32	1871	122	16	0.0060	0.032	55.7
6.50	1.36	1862	131	17	0.0055	0.029	57.6
6.75	1.40	1854	139	18	0.0050	0.027	59.4
7.00	1.44	1846	147	19	0.0045	0.024	61.3
7.25	1.49	1837	156	19	0.0040	0.021	63.1
7.50	0.82	1843	150	16	0.0047	0.040	6.4
7.75	0.85	1837	156	17	0.0047	0.040	6.4

Table 5. Although the ^{137}Cs record (Fig. 3A) does not have clearly resolved peaks that allow accurate independent validation of the ^{210}Pb results, traces of ^{134}Cs detected in the top 1 cm indicate that the high ^{137}Cs activities in the surficial sediments are of Chernobyl origin, in good agreement with the ^{210}Pb dates which place 1986 at a depth of 0.7 cm.

Ľadové pleso

^{210}Pb dates calculated using the CRS model place 1986 at a depth of between 1.25–1.5 cm and are consistent with the ^{137}Cs record (Fig. 3B) which has a sub-surface peak in this section recording fallout from the Chernobyl accident. The ^{210}Pb dates also place 1963 at a depth of 3 cm. Although this is to some extent supported by the presence of traces of ^{241}Am between 0.75–3.5 cm, the lack of precision in the ^{241}Am record does not allow its use in making any correction to the ^{210}Pb dates. The ^{210}Pb chronology, given in detail in Table 6, suggests a background sedimentation rate of between 0.0055–0.0081 g cm^{-2} y^{-1} (0.048–0.075 cm y^{-1}), interrupted by occasional brief episodes of more rapid accumulation most probably caused by land-slips or sediment slumps. The most significant of these events appear to have occurred in the late 19$^{\text{th}}$ century, in the early 1950s, and again during the past year or so. The net effect of these events has been to increase the mean sedimentation rate since the mid 19$^{\text{th}}$ century to 0.012 g cm^{-2} y^{-1} (0.094 cm y^{-1}).

Starolesnianske pleso

^{210}Pb dates calculated using the CRS model place 1986 at a depth of between 1–1.25 cm, and 1963 between 2.5–2.75 cm. Although the ^{137}Cs record (Fig. 3B) does not have distinct sub-surface peaks that accurately validate these dates, the very high ^{137}Cs activities between 0.5–1.75 cm are consistent with the inference that these sediments record fallout from the 1986 Chernobyl accident. Further, traces of ^{241}Am between 1.5–2.75 cm show that sediments from these depths contain fallout from the atmospheric testing of nuclear weapons in the 1960s. The detailed results (Tab. 7) show that sedimentation rates were fairly uniform from the mid 19$^{\text{th}}$ century through to the early 1950s with a mean value during this period of 0.0047 ± 0.0003 g cm^{-2} y^{-1} (0.039 cm y^{-1}), since when there has been a moderate but significant acceleration to a contemporary value of nearly 0.01 g cm^{-2} y^{-1} (0.18 cm y^{-1}).

Table 9. Mean sedimentation rates in the Tatra lake sediment cores.

Site	Core	Mean sedimentation rate		1850 depth	
		g cm^{-2}y^{-1}	cm y^{-1}	g cm^{-2}	cm
Zielowny Staw Gąsienicowy	ZIEL93/1	0.042	0.27		
Długi Staw Gąsienicowy	DLUG93/1	0.0062	0.055	0.89	7.8
Zmarzly Staw Gąsienicowy	GA-1	0.019	0.045	2.87	6.8
Vyšné Temnosmrečinské pleso	TA0019	0.0064	0.060	0.97	9.0
Ľadové pleso	LADO00/1	0.0084	0.067	1.27	10.1
”	LADO00/2	0.013	0.080	1.96	12.0
”	LADO00/3	0.021	0.13	3.18	19.7
”	LADO00/4	0.026	0.055	3.82	8.2
”	LADO00/5	0.014	0.063	2.14	9.5
”	LADO01/6	0.012	0.094	1.8	14.2
Ľadové pleso mean		*0.016*	*0.082*	*2.36*	*12.3*
Starolesnianske pleso	STAR93/2	0.0055	0.050	0.79	7.2
Veľké Hincovo pleso	VHINC01/1	0.018	0.085	2.72	12.8
Nižné Terianske pleso	TERI93/2	0.010	0.048	1.42	6.9
”	TERI96/7	0.0066	0.031	1.0	4.6
Nižné Terianske pleso mean		*0.0083*	*0.040*	*1.21*	*5.8*
Vyšné Wahlenbergovo pleso	FU-1	0.0057	0.043	0.86	6.5

Nižné Terianske pleso

The two cores from Nižné Terianske pleso analysed in detail have very similar radiometric records (Figs 2C, 3C). ^{210}Pb results for both cores suggest intrinsically low sedimentation rates of between 0.004–0.006 g cm^{-2} y^{-1}, but with a major episode of accelerated sedimentation during the period 1920–1930 that appears to be associated with a layer of dense sediment between 3–4.5 cm depth in the 1993 core and 1.4–4 cm in the 1996 core. The very low sedimentation rate in recent decades (in both cores 1986 is placed at around 0.5 cm and 1963 between 1.1–1.7 cm) is supported by the fact that the very high ^{137}Cs concentrations recording Chernobyl fallout were confined to the upper 1 cm of the core, and weapons fallout ^{241}Am to between 0.2–1.5 cm. ^{210}Pb dates for the 1993 core are given in Table 8. The corresponding results for the 1996 core have been given in detail in Appleby (2000) and Šporka et al. (2002).

Gradient cores

These cores, part of the EMERGE work package studying environmental gradients, were analysed in much less detail (4–5 sections per core). Although it was thus not possible to determine detailed chronologies for these cores, mean sedimentation rates could be calculated using the CF:CS model in which exponential regression curves are fitted to the unsupported ^{210}Pb profiles. The results obtained by this method were comparable to those for the master cores, ranging from 0.0057 g cm^{-2} y^{-1} (0.043 cm y^{-1}) in Vyšné Wahlenbergovo pleso to 0.019 g cm^{-2} y^{-1} (0.045 cm y^{-1}) in Zmarzly Staw Gąsienicowy. Mean sedimentation rates for all cores are shown in Table 9. The ^{210}Pb inventories (Tab. 3) show that the relatively high sedimentation rate in Veľké Hincovo pleso 0.018 g cm^{-2} y^{-1} (0.085 cm y^{-1}) is probably due to sediment focussing.

Bulk cores

These cores (from Ľadové pleso) were part of a study analysing the spatial variation of sediment records within a lake (Plöger, 2005). They too were analysed in much less detail (5 samples per core), though since entire inventories were determined they could be dated in the usual way. Mean sedimentation rates (also given in Tab. 9) varied by a factor of three, from 0.0084–0.026 g cm^{-2} y^{-1}. Because of the substantial variations in dry bulk density, the pattern of volumetric sedimentation rates (in cm y^{-1}) was quite different to that of dry mass sedimentation rates (in g cm^{-2} y^{-1}).

Conclusions

The results presented in this paper show that sediments from the study sites generally retain relatively good records of the fallout radionuclides ^{210}Pb and ^{137}Cs, and that these radionuclides can be used to determine reliable dates for the environmental records preserved in these natural archives. As might be expected in such remote, undisturbed sites, sedimentation rates were low, and generally fairly uniform apart from occasional episodes of rapid sedimentation due presumably to land-slips from adjacent steep slopes, or sediment slumps from the margins of the lake. In one case (Zielony Staw Gąsienicowy) such an event appears to have destroyed a significant part of the pre-1950 record. In another (Nižné Terianske pleso), where there was a very low back-ground sedimentation rate, it caused a major distortion of the sediment record. The similarity in the radiometric profiles from the 1993 and 1996 cores shows that records from this site are nonetheless still reliable. The gradient cores show that where detailed chronologies are not required, ‘sketch’ profiles based of a relatively small number of measurements can still provide useful information on the mean sed-

imentation rate. The study of the spatial distribution of sediment records in Ľadové pleso using bulk cores from different parts of the lake show that radionuclide inventories and sedimentation rates may vary significantly over even quite small areas of the lake, and that records from non-dated cores will be reliable only if clear correlations can be obtained with dated cores.

At most of the study sites there were significant discrepancies between the atmospheric fluxes of fallout radionuclides and their supply rates to the lake sediments. The reasons for these discrepancies are not clear, but are presumably related to the fact that much of the fallout occurs during the winter as snow when it is liable to substantial redistribution by the strong winds experienced in these environments. Further, the fraction retained in the surface ice is released quite rapidly during the spring thaw and in some cases may not be retained in the water column. In spite of these problems, dating by ^{210}Pb appears to be quite reliable, suggesting that the impact of these processes is relatively constant from year to year. However, since all atmospherically supplied substances will be similarly affected, these processes must be taken into account when using the sediment records to reconstruct histories of atmospheric pollution.

Acknowledgements

This work has been undertaken in the framework of the AL:PE, MOLAR and EMERGE research projects funded by the European Commission Environment and Climate Programme, Contract Numbers EV5V-CT92-0205, ENV4-CT95-0007, and EVK1-CT 1999–00. It rests on the work of many colleagues in all these projects and their contributions are gratefully acknowledged.

References

Appleby, P.G. 2000. Radiometric dating of sediment records in European mountain lakes. J. Limnol. **59,** Suppl. 1: 1–14.

Appleby, P.G. 2001. Chronostratigraphic techniques in recent sediments, pp. 171–203. In: Last, W.M. & Smol, J.P. (eds) Developments in paleoenvironmental research. Volume 1, Tracking environmental change using lake sediments: Physical and chemical techniques. Kluwer Academic Publisher, Dordrecht.

Appleby, P.G., Nolan, P.J., Gifford, D.W., Godfrey, M.J., Oldfield, F., Anderson, N.J. & Battarbee, R.W. 1986. ^{210}Pb dating by low background gamma counting. Hydrobiologia **141:** 21–27.

Appleby, P.G. & Oldfield, F. 1978. The calculation of ^{210}Pb dates assuming a constant rate of supply of unsupported ^{210}Pb to the sediment. Catena **5:** 1–8.

Appleby, P.G. & Oldfield, F. 1983. The assessment of ^{210}Pb data from sites with varying sediment accumulation rates. Hydrobiologia **103:** 29–35.

Appleby, P.G & Piliposian, G.T. 2004. Efficiency corrections for variable sample height in well-type germanium gamma detectors. Nucl. Inst. & Methods B **225:** 423–433.

Appleby, P.G., Richardson, N. & Nolan, P.J. 1991. ^{241}Am dating of lake sediments. Hydrobiologia **214:** 35–42.

Appleby, P.G., Richardson, N. & Nolan, P.J. 1992. Self-absorption corrections for well-type germanium detectors. Nucl. Inst. & Methods B **71:** 228–233.

Battarbee, R.W., Grytnes, J.-A., Thompson, R., Appleby, P.G., Catalan, J., Korhola, A., Birks, H.J.B., Heegaard, E. & Lami, A. 2002. Comparing palaeolimnological and instrumental evidence of climate change for remote mountain lakes over the last 200 years. J. Paleolimnol. **28:** 161–179.

Goldberg, E.D. 1963. Geochronology with ^{210}Pb, pp. 121–131. In: Radioactive Dating, International Atomic Energy Agency, Vienna.

Krishnaswami, S., Lal, D., Martin, J.M. & Meybeck, M. 1971. Geochronology of lake sediments. Earth Planet. Sci. Lett. **11:** 407–414.

Oldfield, F. & Appleby, P.G. 1984. Empirical testing of ^{210}Pb dating models, pp. 93–124. In: Haworth, E.Y. & Lund, J.G. (eds) Lake sediments and environmental history, Leicester Univ. Press.

Pennington, W., Cambray, R.S. & Fisher, E.M. 1973. Observations on lake sediments using fallout ^{137}Cs as a tracer. Nature **242:** 324–326.

Piliposian, G. & Appleby, P.G. 2003. A model of the impact of winter ice cover on pollutant concentrations and fluxes in mountain lakes. Water, Air, Soil Poll. **44:** 101–115.

Plöger, A. 2005. Measuring and modelling of trace metals and radionuclides in mountain lake systems. PhD Thesis, University of Liverpool.

Robbins, J.A. 1978. Geochemical and geophysical applications of radioactive lead, pp. 285–393. In: Nriagu, J.O. (ed.) Biogeochemistry of lead in the environment, Elsevier Scientific, Amsterdam.

Šporka, F., Štefková, E., Bitušík, P., Thompson, A.R., Agusti-Panareda, A., Appleby, P.G., Grytnes, J.A., Kamenik, C., Krno, I., Lami, A., Rose, N. & Shilland, N.E. 2002. The palaeolimnological analysis of sediments from high mountain lake Nizne Terianske pleso in the high Tatras (Slovakia). J. Paleolimnol. **28:** 95–109.

Wathne, B.M., Patrick, S.T., Monteith, D. & Barth, H. (eds) 1995. AL:PE 1 Report for the period April 1991-April 1993. European Commission DGXII, Luxembourg, 292 pp.

Received June 10, 2005
Accepted May 9, 2006

Appendix. Fallout radionuclide concentrations in Tatra master cores.

Table A.1. Zielony Staw Gąsienicowy core ZIEL93/1.

Depth		^{210}Pb						^{137}Cs	
		Total		Unsupported		Supported			
cm	g cm^{-2}	Bq kg^{-1}	±	Bq kg^{-1}	±	Bq kg^{-1}	±	Bq kg^{-1}	±
0.13	0.00	1474.4	51.5	1409.2	52.1	65.2	7.9	661.2	52.9
1.88	0.18	1044.4	41.8	974.8	42.4	69.6	6.8	703.3	15.9
2.13	0.21	1136.7	38.2	1074.0	38.6	62.7	5.9	820.8	15.5
3.13	0.34	851.8	39.3	749.0	40.0	102.8	7.8	474.4	14.1
4.25	0.52	517.8	26.3	444.7	26.7	73.1	4.6	178.1	6.4
6.25	0.88	479.7	21.1	414.6	21.4	65.1	3.8	133.2	4.9
7.75	1.15	459.4	21.8	396.1	22.1	63.3	3.7	160.9	5.3
8.50	1.29	555.1	26.4	483.6	26.8	71.5	4.3	188.5	6.2
9.50	1.44	465.8	19.2	397.9	19.5	67.9	3.3	122.7	4.4
10.50	1.60	403.2	13.6	333.1	14.0	70.1	3.0	71.8	3.7
11.50	1.76	192.0	15.3	125.9	15.7	66.1	3.5	47.4	3.0
12.50	1.93	150.1	13.1	81.3	13.5	68.8	2.9	24.5	2.4
14.50	2.71	65.7	6.9	−5.2	7.1	70.9	1.7	0.0	0.0
16.50	3.93	40.6	6.6	−7.2	6.9	47.8	1.8	0.0	0.0
18.50	4.76	76.0	9.5	15.9	9.8	60.1	2.2	0.0	0.0
22.50	6.15	65.1	8.2	−4.3	8.5	69.4	2.1	0.0	0.0

Table A.2. Długi Staw Gąsienicowy core DLUG93/1.

Depth		^{210}Pb						^{137}Cs	
		Total		Unsupported		Supported			
cm	g cm^{-2}	Bq kg^{-1}	±	Bq kg^{-1}	±	Bq kg^{-1}	±	Bq kg^{-1}	±
0.13	0.00	1213.6	53.8	1164.0	54.3	49.6	7.4	1282.8	6.3
0.38	0.02	925.8	82.5	802.7	84.2	123.1	16.7	1290.4	30.3
0.63	0.04	942.1	30.2	887.5	30.6	54.6	4.7	1281.6	15.2
1.13	0.10	559.1	33.0	511.9	33.6	47.2	6.6	696.6	13.5
1.38	0.13	575.2	30.4	525.9	30.9	49.3	5.5	562.4	13.6
2.13	0.22	386.1	21.7	338.4	22.2	47.7	4.3	273.4	8.1
2.88	0.31	356.2	29.3	302.8	30.0	53.4	6.4	157.0	7.4
3.63	0.40	340.1	31.0	276.3	32.1	63.8	8.4	118.1	8.3
4.25	0.47	150.9	13.5	101.3	13.8	49.6	2.9	51.8	2.9
5.25	0.59	142.5	11.5	80.6	11.9	61.9	3.0	30.0	3.2
5.75	0.64	73.0	11.5	17.9	11.8	55.1	2.9	18.4	2.6
6.25	0.70	53.2	7.6	−3.4	8.0	56.6	2.4	22.8	2.0
6.75	0.76	70.5	7.1	15.6	7.3	54.9	1.7	16.5	1.4
7.25	0.82	75.0	10.7	25.2	11.0	49.8	2.2	15.7	1.7
8.50	0.97	66.8	7.9	12.9	8.2	53.9	2.1	8.9	2.0
10.50	1.22	50.4	7.0	−3.6	7.2	54.0	1.7	5.5	1.2
12.50	1.53	43.6	9.4	−1.1	9.7	44.7	2.3	0.5	1.6
14.50	1.73	37.5	7.8	−5.3	8.0	42.8	2.0	1.6	1.9

Table A.3. Ľadové pleso core LAD01/6.

Depth		^{210}Pb						^{137}Cs		^{241}Am	
		Total		Unsupported		Supported					
cm	g cm^{-2}	Bq kg^{-1}	±	Bq kg^{-1}	±	Bq kg^{-1}	±	Bq kg^{-1}	±	Bq kg^{-1}	±
0.38	0.04	51.5	14.4	7.3	14.9	44.2	3.7	44.5	4.1	0.0	0.0
0.88	0.10	1351.4	51.3	1300.2	51.6	51.2	6.3	1031.2	16.0	4.8	3.0
1.38	0.17	1340.5	56.2	1298.7	56.6	41.8	6.6	1251.0	18.6	7.8	4.8
1.88	0.23	699.8	38.0	658.9	38.5	40.9	6.1	886.6	17.6	5.9	3.8
2.38	0.29	650.9	32.7	590.9	33.4	60.0	6.9	864.8	15.2	8.9	3.1
3.38	0.44	293.7	15.1	264.4	15.4	29.3	3.2	324.2	6.2	4.6	1.6
4.38	0.59	126.9	15.5	74.7	16.0	52.2	3.9	138.6	5.5	0.0	0.0
5.25	0.70	260.6	18.6	203.6	19.1	57.0	4.5	206.9	5.6	0.0	0.0
6.25	0.83	148.2	14.1	113.6	14.3	34.7	2.5	89.7	2.8	0.0	0.0
7.25	0.95	153.6	13.9	112.8	14.2	40.8	2.9	46.5	3.3	0.0	0.0
8.25	1.08	152.6	12.1	109.8	12.5	42.7	2.9	28.7	2.5	0.0	0.0
9.25	1.22	105.3	12.7	64.3	13.0	41.0	2.9	12.1	2.0	0.0	0.0
10.25	1.35	39.9	11.9	−1.5	12.1	41.4	2.3	6.1	1.7	0.0	0.0
11.25	1.46	70.9	10.1	29.0	10.4	41.8	2.5	18.6	2.3	0.0	0.0
12.25	1.56	60.8	9.9	20.1	10.1	40.7	2.3	38.5	2.1	0.0	0.0
13.25	1.67	76.0	10.2	34.2	10.6	41.8	2.8	31.2	2.2	0.0	0.0
14.25	1.78	65.1	12.2	30.6	12.5	34.5	2.3	22.4	2.0	0.0	0.0
15.25	1.90	36.2	6.2	−0.3	6.4	36.5	1.7	16.5	1.3	0.0	0.0
16.25	2.02	49.3	6.6	18.3	6.8	31.0	1.6	20.5	1.3	0.0	0.0

Table A.4. Starolesnianske pleso core STAR93/2.

Depth		^{210}Pb						^{137}Cs		^{241}Am	
		Total		Unsupported		Supported					
cm	g cm^{-2}	Bq kg^{-1}	±	Bq kg^{-1}	±	Bq kg^{-1}	±	Bq kg^{-1}	±	Bq kg^{-1}	±
0.63	0.02	1273.6	47.4	1229.0	48.0	44.6	7.4	5582.9	8.4	13.1	3.0
1.13	0.06	1251.5	88.9	1212.8	89.3	38.7	7.7	5694.5	63.1	0.0	0.0
1.63	0.11	1196.3	42.6	1163.4	43.1	32.9	6.6	4365.3	34.1	17.3	3.0
2.13	0.16	931.4	32.7	886.9	33.4	44.5	6.7	2176.7	20.4	10.6	2.5
2.63	0.22	856.4	40.2	808.1	40.6	48.3	6.1	1186.7	17.8	9.1	2.6
3.13	0.29	809.4	32.4	758.1	32.9	51.3	6.0	811.1	14.7	0.0	0.0
3.63	0.35	695.3	62.1	650.1	62.5	45.2	7.1	438.8	16.8	0.0	0.0
4.25	0.43	410.8	21.3	371.8	21.5	39.0	3.4	236.5	7.7	0.0	0.0
5.25	0.55	146.9	9.8	110.1	10.2	36.8	2.7	179.6	3.6	0.0	0.0
6.25	0.67	91.8	12.4	53.2	12.7	38.6	2.9	75.9	3.2	0.0	0.0
7.25	0.79	59.7	7.2	21.4	7.6	38.3	2.3	57.5	2.9	0.0	0.0
8.50	0.94	46.4	7.7	14.1	7.8	32.3	1.5	42.4	1.6	0.0	0.0
10.50	1.18	30.9	5.3	2.2	5.6	28.7	1.7	18.2	1.9	0.0	0.0
12.50	1.40	29.1	7.8	0.3	7.9	28.8	1.4	15.0	1.1	0.0	0.0

Table A.5. Nižné Terianske pleso core TERI93/2.

Depth		^{210}Pb						^{137}Cs	
		Total		Unsupported		Supported			
cm	g cm^{-2}	Bq kg^{-1}	±	Bq kg^{-1}	±	Bq kg^{-1}	±	Bq kg^{-1}	±
0.13	0.00	2670.3	148.6	2622.8	149.9	47.5	19.0	2966.4	23.7
0.88	0.06	921.6	47.3	865.0	47.9	56.5	7.6	1727.2	25.1
1.13	0.10	703.1	31.0	653.6	31.6	49.6	5.9	930.5	12.8
1.63	0.20	598.3	32.3	541.0	32.9	57.3	6.4	599.9	11.3
2.13	0.30	422.6	47.6	280.3	49.5	142.2	13.6	261.3	14.1
2.63	0.39	206.1	23.4	135.8	24.0	70.3	5.6	51.6	5.3
3.13	0.51	166.8	12.7	118.2	13.0	48.6	3.0	17.2	3.3
3.38	0.59	120.2	11.5	68.1	11.8	52.1	2.5	19.0	2.2
4.25	0.86	70.2	5.9	40.1	6.0	30.1	1.3	2.4	0.8
5.25	1.11	118.9	8.9	74.1	9.2	44.7	2.1	7.8	1.6
6.25	1.32	78.2	8.4	35.8	8.6	42.4	1.8	0.3	1.2
7.25	1.49	69.0	7.1	19.0	7.4	50.0	1.8	1.8	1.8
8.50	1.74	38.3	7.6	−2.0	7.8	40.3	1.7	3.8	1.2
10.50	2.10	40.7	9.1	−3.9	9.3	44.6	2.0	5.8	1.4
12.50	2.35	44.4	11.8	−3.2	12.0	47.6	2.4	14.6	2.1
14.50	2.58	34.7	9.5	−8.0	9.8	42.7	2.2	6.3	1.9

Table A.6. Nižné Terianske pleso core TERI96/7.

Depth		^{210}Pb						^{137}Cs		^{241}Am	
		Total		Unsupported		Supported					
cm	g cm^{-2}	Bq kg^{-1}	±	Bq kg^{-1}	±	Bq kg^{-1}	±	Bq kg^{-1}	±	Bq kg^{-1}	±
0.10	0.01	2118.9	92.9	2049.3	94.0	69.5	14.2	2362.0	49.5	0.0	0.0
0.30	0.02	1584.2	42.0	1526.0	42.3	58.2	5.1	2206.9	22.6	8.0	2.8
0.50	0.05	1262.4	75.7	1216.5	76.2	45.8	8.2	1459.6	31.0	10.9	3.1
0.90	0.10	856.7	43.3	806.4	43.7	50.3	5.7	987.2	16.3	8.5	3.0
1.30	0.17	615.3	40.7	574.5	41.3	40.8	6.7	653.0	18.6	3.7	1.9
1.70	0.27	213.9	15.8	171.5	16.1	42.5	3.3	168.1	5.3	0.0	0.0
2.10	0.40	140.2	8.3	98.7	8.5	41.5	2.0	89.2	2.9	0.0	0.0
2.50	0.54	120.4	12.2	80.4	12.4	40.0	2.2	40.2	2.4	0.0	0.0
2.90	0.63	125.9	12.9	71.2	13.4	54.8	3.7	14.3	3.8	0.0	0.0
3.30	0.72	128.2	11.2	81.6	11.4	46.6	1.9	18.8	1.8	0.0	0.0
3.70	0.81	120.9	11.1	69.8	11.4	51.2	2.5	22.4	1.9	0.0	0.0
4.10	0.90	174.5	19.4	94.4	20.1	80.2	5.3	12.8	5.4	0.0	0.0
4.30	0.94	59.3	9.1	13.1	9.3	46.2	2.3	5.5	2.2	0.0	0.0
4.50	0.97	100.9	16.5	45.0	17.0	55.9	4.1	7.8	3.6	0.0	0.0
4.70	1.00	71.6	14.1	26.3	14.5	45.3	3.2	17.7	3.0	0.0	0.0
4.90	1.03	81.9	9.7	38.5	10.0	43.4	2.7	20.5	2.9	0.0	0.0
5.10	1.07	68.0	16.6	7.0	16.9	60.9	3.1	14.4	2.4	0.0	0.0
5.30	1.10	52.2	14.7	3.3	15.0	48.9	3.3	10.7	2.9	0.0	0.0
5.50	1.13	73.6	14.6	23.7	14.9	49.9	2.7	13.2	2.3	0.0	0.0
5.70	1.17	52.2	13.0	−8.6	13.4	60.8	3.1	7.7	2.0	0.0	0.0
5.90	1.20	47.3	8.8	0.6	9.2	46.7	2.4	7.7	2.4	0.0	0.0
8.10	1.64	40.7	9.5	−6.5	9.8	47.2	2.3	18.4	2.2	0.0	0.0
11.90	2.11	29.8	9.2	−18.1	9.8	47.9	3.3	5.9	3.5	0.0	0.0